Diagn Interv Radiol 2022; DOI: 10.5152/dir.2022.201007

ABDOMINAL IMAGING

ORIGINAL ARTICLE

Prognostic role of iodine values for gastric cancer after neoadjuvant chemotherapy: a strong independent prognostic factor

Yang Zhang
Junfa Chen
Fei Yuan
Benyan Zhang
Bei Ding
Huan Zhang

PURPOSE
We aimed to systematically explore the value of iodine values calculated from dual-energy computed tomography (DECT) as potential prognostic factors for locally advanced gastric cancer (LAGC) patients undergoing neoadjuvant chemotherapy (NAC).

METHODS
Eighty-five LAGC patients were examined using DECT before and after NAC and were divided into responders and non-responders based on the tumor regression grade (TRG). The iodine values including portal- and delayed-phase iodine uptake (IU_p and IU_d, mg/mL) and total iodine uptake (TIU_p and TIU_d, mg) were acquired. Correlations between the reduction ratios of iodine values and TRG were analyzed. The diagnostic performance of parameters for differentiating responders from non-responders was calculated. Kaplan–Meier method was used for survival analysis.

RESULTS
The reduction ratios of total iodine uptake ($\%\Delta TIU_p$ and $\%\Delta TIU_d$) were significantly correlated with TRG ($P < .001$). The ypN stage, $\%\Delta TIU_p$, and $\%\Delta TIU_d$ were significant factors influencing progression-free survival (PFS) ($P < .050$). A value of $\%\Delta TIU_d \leq 62.19\%$ was associated with negative prognosis [relative risk (RR):2.103; $P = 0.021$], as was ypN stage (RR: 4.250; $P = .003$).

CONCLUSION
Iodine values (especially the TIU) are noninvasive quantitative parameters that are potentially helpful for evaluating the treatment response and survival prognosis of LAGC after NAC. $\%\Delta TIU_d$ represents a strong independent prognostic factor, increasing preoperative risk assessment performance.

The incidence and mortality of gastric cancer (GC) are very high in the world.[1,2] Eighty to 90 percent[3] of these patients were diagnosed as having locally advanced gastric cancer (LAGC), which has a poor prognosis primarily due to recurrence after surgery. Neoadjuvant chemotherapy (NAC) is a safe treatment modality that appears to have many advantages: it reduces tumor stage and size, increases the R_0 resection rate, and significantly improves survival.[4-6]

The assessment of prognosis after NAC can help to timely adjust the therapeutic regimens and to avoid potential toxicity. Therefore, the identification of preoperatively prognostic biomarkers is important. p53 codon 72 polymorphism[7] in blood samples from LAGC patients after NAC and some immunohistochemistry biomarkers, such as thymidylate synthase,[8] C-C motif chemokine 22,[9] and orphan nuclear receptor,[10] were considered to be independent prognostic factors. Other studies[11,12] found that immune-inflammation indicators are associated with survival. After assessing the clinical-pathologic variables (including ypT, ypN, ypTNM stage, complications, and perineural or vascular invasion),[10,13-15] lymph node status after NAC was established to be an independent prognostic factor. However, preoperative imaging prognostic factors of NAC, which identify the LAGC patients who are potential possibly to benefit from it, are limited at present.

With the rapid development of imaging technology, dual-energy computed tomography (DECT) has become an important technological milestone. Specifically, it uses 2 acquisitions

From the Cancer Center, Department of Radiology (Y.Z., J.C.), Zhejiang Provincial People's Hospital, Affiliated People's Hospital, Hangzhou Medical College, Hangzhou, Zhejiang, China; Department of Radiology (Y.Z., B.D., H.Z. ✉ huanzhangy@163.com), and Department of Pathology (F.Y., B.Z.), Shanghai Jiao Tong University School of Medicine, Ruijin Hospital, Shanghai, China.

Received 23 December 2020; revision requested 26 January 2021; last revision received 3 May 2021; accepted 17 May 2021.

Publication date: 10 August 2022.

DOI: 10.5152/dir.2022.201007

You may cite this article as: Zhang Y, Chen J, Yuan F, Zhang B, Ding B, Zhang H. Prognostic role of iodine values for gastric cancer after neoadjuvant chemotherapy: a strong independent prognostic factor. *Diagn Interv Radiol.* 2022;28(5):388-395.

with X-ray spectra that differ in their mean photon energies to gain additional information on the scanned material. Based on the material decomposition algorithm from DECT,[16,17] quantitative material concentrations can be obtained, including iodine uptake (IU, mg/mL) and total iodine uptake (TIU, mg). Our previous research[18] found that the reduction ratios of tumor TIU in the portal phase were helpful to predict the pathological regression and may be a valuable potential predictor of progression-free survival in LAGC after NAC. However, we only analyzed TIU in the portal phase. Along with an improvement in the vascular enhancement, the tumor contrast-to-noise ratio was remarkably improved. In addition, enhanced scanning showed that LAGC lesions were continuously enhanced layer by layer from inside to outside. Whether iodine values (IU and TIU) from the portal phase and delayed phase can be used as independent prognostic factors for LAGC patients after NAC has not yet been fully evaluated.

Therefore, this study was aimed to systematically explore the value of iodine values calculated from DECT as potential prognostic factors for LAGC patients after NAC.

Methods

Patients

The institutional review board approved this retrospective study and waived the requirement for informed consent (No. 201688). All procedures involving human adhere to the principles of the Declaration of Helsinki.

From April 2013 to March 2017, 132 patients were enrolled in our protocol. The inclusion criteria included the following: (a) a visible tumor defined as $cT_{2\text{-}4a/b}N_xM_0$ on DECT images; (b) a preliminary diagnosis of Borrmann type I to Borrmann type III without previous chemotherapy; (c) standard NAC before surgery and radical resection; (d) histologically proven gastric adenocarcinoma; and (e) adequate hepatic, renal, and hematologic function. Forty-seven patients were excluded for the following reasons: (a) a history of other malignancies (1 colon tumor and 1 rectal tumor, n = 2); (b) insufficient DECT images (such as movement artifacts, n = 6); (c) Siewert type I tumors (n = 16); (d) the presence of peritoneal metastases in intraoperative exploration (n = 5); (e) discontinuation of NAC due to side effects (n = 10); and (f) less than 1-month follow-up (n = 8). Ultimately, 85 patients were enrolled in this study.

Main points

- Iodine values (especially the total iodine uptake) are noninvasive quantitative parameters that are potentially helpful for evaluating the treatment response and survival prognosis of gastric cancer after neoadjuvant chemotherapy.
- The reduction ratio of total iodine uptake in the delayed phase represents a strong independent prognostic factor, increasing preoperative risk assessment performance.
- The reduction ratio of total iodine uptake can serve to guide patients toward individual treatment and predict the prognosis.

Chemotherapy

In this study, our neoadjuvant chemotherapy regimen was strictly in accordance with the MAGIC protocol,[19] including intravenous infusion of epirubicin, cisplatin, and fluorouracil. Usage and dosage are 50 mg/m^2 epirubicin on day 1, 60 mg/m^2 cisplatin on day 1, and 200 mg/m^2/day fluorouracil on days 1–21, respectively. The same regimen was used before and after neoadjuvant chemotherapy for 3 cycles.

DECT protocol

All patients underwent DECT exams 1 week before the beginning of NAC and within 2 weeks after completion of the third cycle of NAC using the same second-generation DECT scanner (Siemens SOMATOM Definition Flash; Siemens Medical Solutions). After overnight fasting, the patient drank 1000-1500 mL of water and was injected with a hypotonic agent (20 mg of scopolamine) to distend the stomach before DECT scanning. The tube voltages were 100/Sn140 kV with a tin filter using references of 230 and 178 mA. The collimator was 128 × 0.6 mm. The pitch was 0.6. All acquisitions were obtained in real-time by the automatic dose modulation protocol (CareDose 4D; Siemens Medical Solutions). To estimate the time to the peak enhancement of the celiac trunk, 16 mL contrast agent was first injected as a test bolus. Then, the same contrast agent (1.5 mL iopromide per kilogram of body weight, Ultravist 370; Schering) was injected at a rate of 3 mL/s. Three-phase enhanced DECT scanning was performed. The arterial phase was scanned to observe peri-gastric arteries when the celiac trunk peak enhancement appeared. The portal phase was scanned after 20 s of celiac trunk peak enhancement, and the delayed phase was scanned after 150 s of contrast agent injection. The portal- and delayed-phase images were used to observe the tumor.

Image analysis

Two gastrointestinal radiologists with more than 15 years of experience independently analyzed all DECT images. Both of them knew that the enrolled patients had endoscopically confirmed GC, but they were completely blinded to the other clinicopathological features, such as size, location, staging, and so on.

Figure 1 shows the process of image analysis using the offline prototype software eXamine (eXamine Prototype, Siemens Healthcare Sector). The two radiologists initially measured 15 patients before the actual reading, and intraclass correlation coefficients (ICC) greater than 0.750 indicated that the observers were familiar with the software and that the data were reliable and representative. Then, the portal- and delayed-phase images of all patients were transmitted to the software. The two radiologists independently analyzed each DECT scan without knowing whether the scan was pre- or post-treatment. This software semiautomatically segments the entire tumor and identifies the volume of interest (VOI) of the primary tumor by drawing a straight line through the tumor.[18] If the semiautomatically identified area is unsatisfactory, the VOI can be manually adjusted. After that, IU (mg/mL) and TIU (mg) were calculated from the entire tumor's VOI using this software by the tumor segmentation algorithm.[20] This algorithm can transform spectral information of dual-energy data into iodine values based on the calibration measurements made by the manufacturer. In addition to quantification, the software also provides visualization iodine maps. Among them, IU (mg/mL) represents the iodine uptake concentration per unit volume of the whole tumor, and TIU (mg) represents the total iodine uptake of the whole tumor. Finally, we obtained iodine values, including portal- and delayed-phase iodine uptake (IU_p and IU_d, mg/mL) and total iodine uptake (TIU_p and TIU_d, mg). For the purposes of this study, the measurements obtained by the

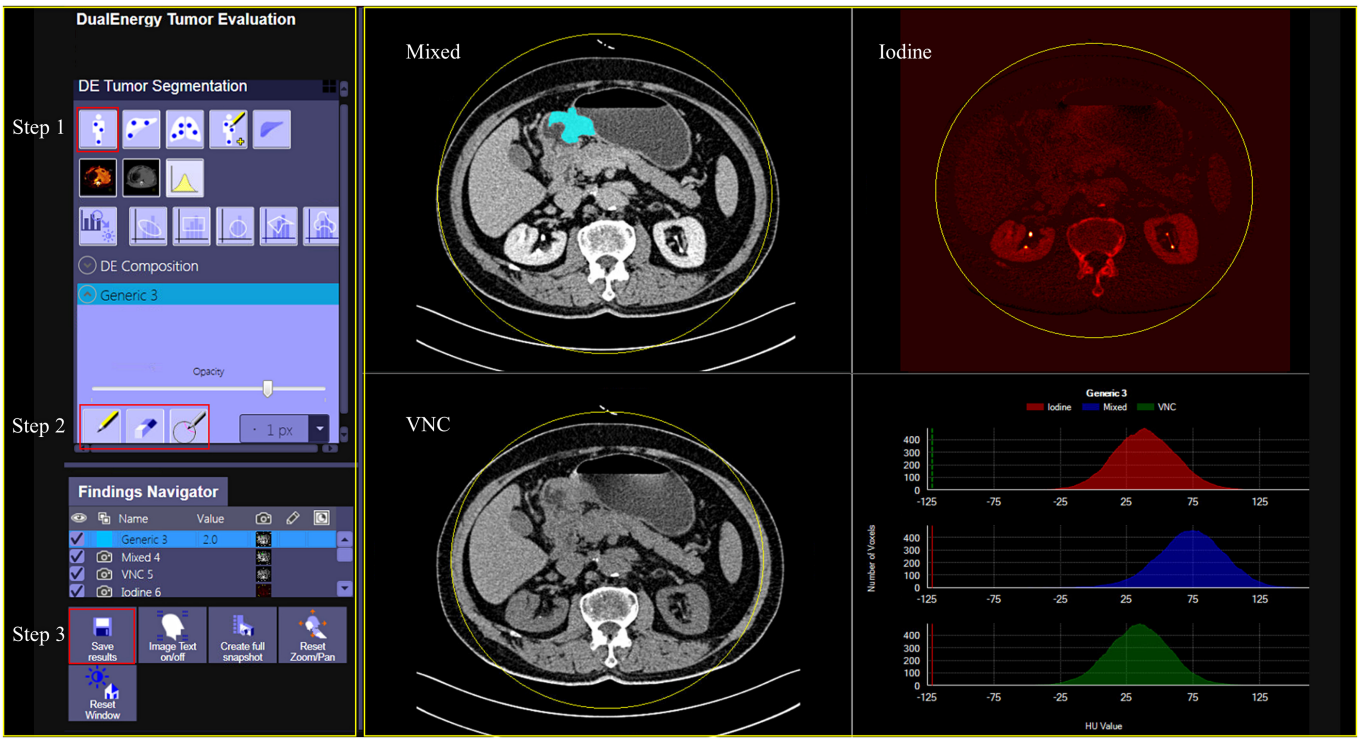

Figure 1. The process of image analysis using the offline prototype software. The visualization images, including mixed energy image, iodine map and virtual non-contrasted (VNC) image, and the distribution of density values of the identified lesion, are on the right. The operation interface of this software is on the left. Step 1: The target lesion was semiautomatically segmented in 3D and with color-labeled tumor displayed on the representative axial slice. Step 2: If the semiautomatically identified area was unsatisfactory, the volume of interest (VOI) can be manually adjusted. Step 3: Save the iodine values calculated from the entire tumor's VOI by the tumor segmentation algorithm.

2 radiologists were averaged for further analysis. The following formulae were used to calculate the reduction ratios in iodine values between the 2 DECT examinations:

$\%\Delta IU_p = (IU_p\text{-before} - IU_p\text{-after})/IU_p\text{-before} \times 100\%$

$\%\Delta IU_d = (IU_d\text{-before} - IU_d\text{-after})/IU_d\text{-before} \times 100\%$

$\%\Delta TIU_p = (TIU_p\text{-before} - TIU_p\text{-after})/TIU_p\text{-before} \times 100\%$

$\%\Delta TIU_d = (TIU_d\text{-before} - TIU_d\text{-after})/TIU_d\text{-before} \times 100\%$

("-before" represents pretreatment and "-after" represents post-treatment)

Surgery, histopathological evaluation, and follow-up

Patients underwent total gastrectomy or subtotal gastrectomy with D2 lymphadenectomy after NAC.

Two pathologists independently analyzed the surgical specimens for the depth of gastric wall invasion (ypT), the involvement of regional lymph nodes (ypN), tumor regression grading (TRG), and the histological subtypes. The definitions for ypT and ypN staging were determined in accordance with the pathologic TNM staging system.[21] Tumor response to NAC was evaluated according to the histopathologic regression, namely, Becker's TRG system[22,23] which is widely used as the gold standard.

Becker's TRG system classifies tumor response into 3 categories based on the percentage of residual tumors in the primary tumor bed. Grade 1, <10%; grade 2, 10%-50%; and grade 3, >50%. Differences in the evaluation were resolved by consensus. We treated grade 1 patients as responders and grades 2 or 3 patients as non-responders in the subsequent analysis.

In the first year, patients were examined every 3 months, in the second year every 6 months, and thereafter every year until the fifth year. Follow-up procedures included physical examination, tumor marker measurement, chest x-rays, endoscopy, and computed tomography (CT) scans.[24] Progression-free survival (PFS) is often used as the primary endpoint in cancer clinical trials and refers to the length of time from randomization to the first event (local recurrence, distant metastasis, or death or the last follow-up date).

Statistical analysis

Statistical analyses were performed using Statistical Package for the Social Sciences Statistical Software (version 24.0; SPSS, USA) and Medcalc Statistical Software (version 17.9.4; Medcalc). ICC was used to evaluate the interclass agreement of the 2 radiologists. The differences between TRG (grade 1, grade 2, and grade 3) and the quantitative parameters ($\%\Delta IU_p$, $\%\Delta IU_d$, $\%\Delta TIU_p$, and $\%\Delta TIU_d$) were evaluated by one-way analysis of variance or Kruskal–Wallis tests according to the results of normality analysis. The associations between TRG and the 4 parameters were evaluated by Spearman's correlations. The diagnostic performance of the 4 parameters for predicting histologic regression was evaluated by receiver operating characteristic (ROC) curves. Differences in performance were analyzed by comparing the area under the receiver operating characteristic curve (AUC) using DeLong test. The threshold was chosen according to the point nearest to the upper left corner in the ROC curves. According to the thresholds for the various parameters calculated by ROC analysis, we divided all patients into responder (greater than the threshold) and non-responder (less than or equal to the

threshold) groups. Survival analysis was performed using the Kaplan–Meier method, and the log-rank test was used to calculate PFS rates, to draw the survival curves, and to evaluate the associations between the different groups and PFS. Then, the Cox regression model was used to assess the independent risk factors for PFS. All tests were 2-sided, and $P < .050$ was regarded as significant.

Table 1. The inter-rater reliability of the measurement between the 2 readers

	IU_p-before	IU_p-after	IU_d-before	IU_d-after
ICC (95% CI)	0.934 (0.900, 0.957)	0.925 (0.886, 0.950)	0.931 (0.896, 0.955)	0.924 (0.886, 0.950)
	TIU_p-before	TIU_p-after	TIU_d-before	TIU_d-after
ICC (95% CI)	0.918 (0.877, 0.946)	0.903 (0.854, 0.936)	0.901 (0.851, 0.934)	0.894 (0.842, 0.930)

An ICC greater than 0.750 indicated good agreement.
ICC, intraclass correlation coefficient.

Results

Eighty-five LAGC patients (55 male, 30 female; mean age ± standard deviation, 59 years ± 9; age range: 39-81 years) were enrolled in our study. Among the 85 patients, tumors were in the cardia (n = 13), fundus (n = 6), body (n = 22), antrum (n = 31), cardia and body (n = 6), or antrum and body (n = 7) of the stomach. Total gastrectomy was carried out in 60 cases and subtotal gastrectomy in 25 cases. According to the histological subtypes, they were divided into differentiated adenocarcinoma (n = 40) and undifferentiated adenocarcinoma (n = 45). Among the 85 patients, there were 34 cases of grade 1, 26 cases of grade 2, and 25 cases of grade 3 regression.

There was significant interclass consistency between the iodine values of the 2 radiologists (ICC: 0.894-0.934, Table 1).

Figures 2a and 2b show the distribution of various parameters at different histopathological grades. The percentage changes in iodine values revealed marked differences with TRG ($P < .010$). The correlation was highest for $\%\Delta TIU_p$ (Spearman's correlation coefficient, $rs = -0.550$, $P < .001$), followed by $\%\Delta TIU_d$ ($rs = -0.508$, $P < .001$), $\%\Delta IU_p$ ($rs = -0.443$, $P < .001$), and $\%\Delta IU_d$ ($rs = -0.304$, $P = .005$). The details of the results are presented in Table 2.

ROC analysis was performed on the 4 parameters at various cutoff levels to differentiate responders (grade 1) from non-responders (grade 2 or 3). $\%\Delta TIU_p$ showed a higher AUC than did $\%\Delta TIU_d$ and $\%\Delta IU_p$ (AUC: 0.796 vs. 0.780 and 0.691, respectively), although the differences between the AUCs were not significant (Figure 2c). In addition, $\%\Delta TIU_p$ showed higher sensitivity than did $\%\Delta TIU_d$ and $\%\Delta IU_p$ (sensitivity: 85.29% vs. 76.47% and 64.71%, respectively). The specificities of the three parameters were slightly different (68.63% for $\%\Delta TIU_p$, 66.67% for $\%\Delta TIU_d$, and 70.59% for $\%\Delta IU_p$). The AUC of $\%\Delta IU_d$ was the lowest (AUC = 0.624) but the difference was not significant ($P = .061$). The details of the results are presented in Table 3.

The follow-up period was 5-59 months. For all patients, the median follow-up was 17 months with a mean follow-up of 20 months. During the observation period, 43 of the 85 patients experienced tumor recurrence, metastasis, or death. The median follow-up was 13 months with a mean follow-up of 14 months. For 42 of the 85 patients without tumor recurrence or metastasis, the median follow-up was 22 months with a mean follow-up of 26 months.

By univariate analysis, $ypN_{1\text{-}3}$ staging [hazard ratio (HR): 4.549; 95% CI: 2.453-8.435; $P < .001$] (Figure 3a), $\%\Delta TIU_d$ (HR: 2.361; 95% CI: 1.293-4.310; $P = .005$) (Figure 3b), and $\%\Delta TIU_p$ (HR: 1.829; 95% CI: 0.996-3.360; $P = .041$) were significant factors influencing PFS, whereas the sex ($P = .736$) and age ($P = .315$) of the patients, ypT staging ($P = .102$), histological subtype ($P = .591$), $\%\Delta IU_p$ ($P = .073$), and $\%\Delta IU_d$ ($P = .226$) were not significantly correlated with PFS. The details of the univariable analysis results for PFS are summarized in Table 4.

Multivariate analysis revealed that $ypN_{1\text{-}3}$ staging [relative risk (RR): 4.250; 95% CI: 1.661-10.877; $P = .003$] and $\%\Delta TIU_d$ (RR: 2.103; 95% CI: 1.119-3.952; $P = 0.021$) were independent prognostic factors for PFS. Figures 4 and 5 represent the DECT images of a responder and a non-responder, respectively.

Discussion

In this study, the TRG system was used as the gold standard to group patients. Our results suggested that the change rates of iodine values were useful for assessing the treatment response of LAGC to NAC. In addition, the %ΔTIU was more valuable than %ΔIU in evaluating potential prognosis for LAGC patients after NAC. We demonstrated that more than a 60.80% reduction in tumor TIU_p or more than a 62.19% reduction in tumor TIU_d can serve to guide LAGC patients toward surgery and can indicate a positive prognosis. Our most important finding was that $\%\Delta TIU_d$ represented a strong independent prognostic factor for PFS (RR: 2.103). Therefore, iodine values (especially the TIU) are non-invasive quantitative parameters that are potentially helpful for evaluating the treatment response and survival prognosis of LAGC after NAC.

Several studies have focused on the value of IU to evaluate the effect of treatment in glioma[25] and cervical cancer.[26] However, no more than 35 cases were enrolled in these studies, and the gold standards were traditional anatomical standards, not histopathologic regression. Therefore, the results are challengeable and unconvincing. Previously published studies have suggested that immune-inflammation indicators[11,12] and immunohistochemistry biomarkers[8-10] can be used as independent prognostic factors in GC patients after NAC. However, the exact mechanisms of immune-inflammation indicators remain unclear, and immunohistochemical biomarkers are usually expensive and time-consuming.[15] One report[27] about MRI found that the apparent diffusion coefficient value of the lesion was an independent prognostic indicator. However, only 28 GC patients who underwent NAC were enrolled in this study and MRI cannot be routinely used for preoperative scanning. On the other hand, a CT scan was recommended not only for preoperative GC staging and for determining resectability[28] but also for choosing the candidates suitable for NAC.[29]

Texture analysis, as a hot topic for quantitative imaging, has been receiving much attention. Two studies on treated GC found that texture analysis can predict therapy response[30] and prognosis.[31] Nevertheless, lacking uniform recommendation regarding

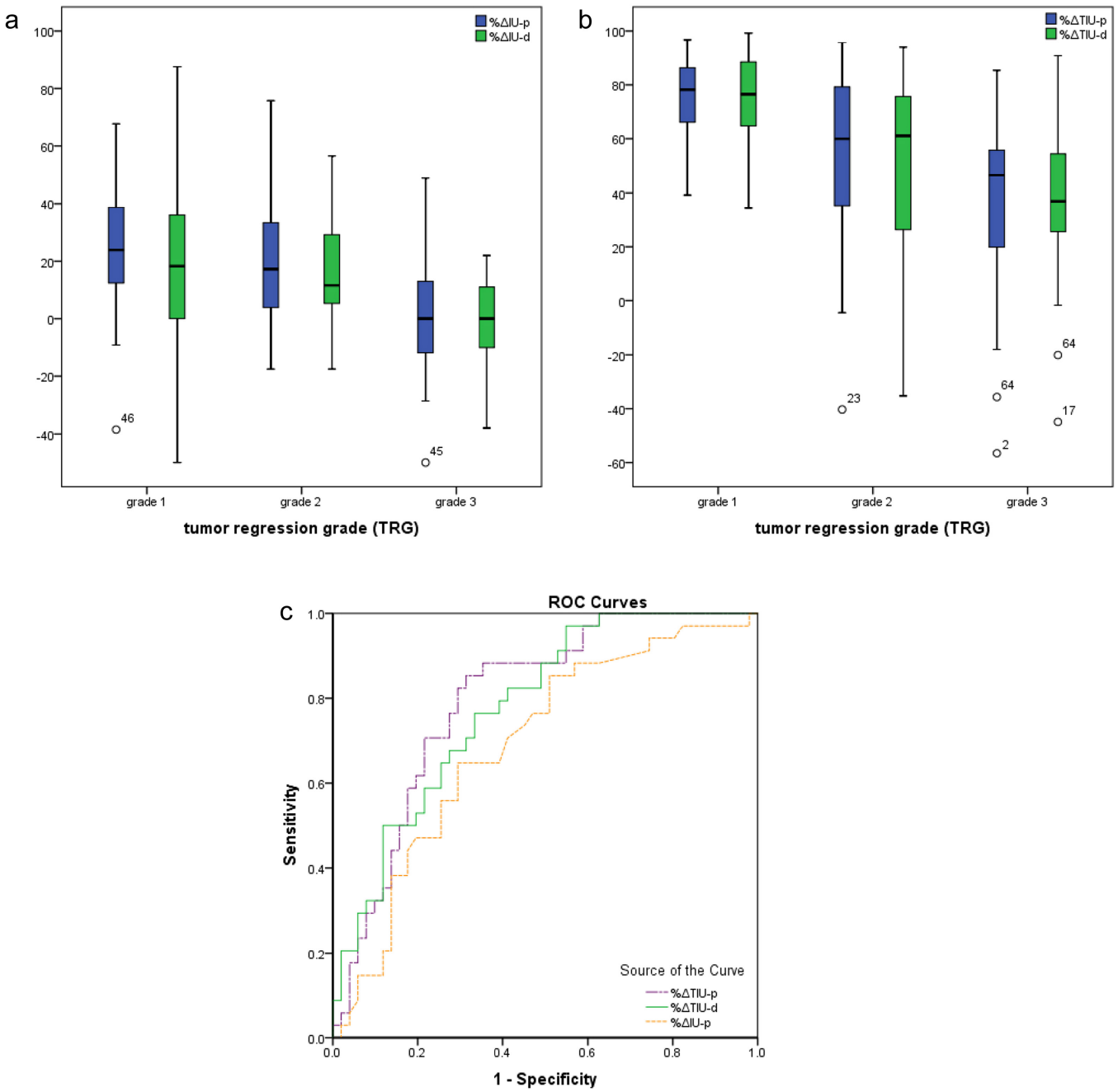

Figure 2. a-c. **(a)** Boxplots show $\%\Delta IU_p$ and $\%\Delta IU_d$ with tumor regression grade (TRG). **(b)** Boxplots show $\%\Delta TIU_p$ and $\%\Delta TIU_d$ with TRG. **(c)** Graph displaying receiver operating characteristic curves (ROCs) of $\%\Delta TIU_p$, $\%\Delta TIU_d$ and $\%\Delta IU_p$ in discriminating responders (grade 1) and non-responders (grade 2 or 3) on the basis of TRG.

Table 2. The performance of different parameters in evaluating histopathological regression

Parameter	Grade 1 (n = 34)	Grade 2 (n = 26)	Grade 3 (n = 25)	P^a	Correlation coefficient (rs)[b]	*P* for Spearman[b]
$\%\Delta IU_p$	25.592 ± 21.708	22.143 ± 23.060	−0.390 ± 20.754	.000	−0.443	.000
$\%\Delta IU_d$	18.311 (36.259)	11.652 (26.678)	0.000 (24.646)	.008	−0.304	.005
$\%\Delta TIU_p$	78.250 (21.550)	59.959 (47.596)	46.561 (40.606)	.000	−0.550	.000
$\%\Delta TIU_d$	76.535 (25.341)	61.093 (49.995)	36.902 (33.136)	.000	−0.508	.000

Mean ± standard deviation or median (interquartile range) are given.
[a]*P* value was determined by one-way analysis of variance (ANOVA) or Kruskal–Wallis tests according to the results of normality analysis; [b]rs determined with correlation coefficient for Spearman's correlation analysis.

the CT phase for texture analysis and the obvious variability in methods and post-processing techniques limit the wide use.[32] Our previous study[18] found that $\%\Delta TIU_p$ may be one of the potentially valuable predictive parameters for LAGC after NAC. However, this study only preliminarily analyzed the TIU in the portal phase. IU was not involved, and the value of the delayed phase was not discussed. Thus, there is still room for improvement to predict pathological response and survival in LAGC patients after NAC.

Table 3. Diagnostic performance of parameters to differentiate responders from non-responders by ROC analysis

Parameter	AUC (95% CI)	Threshold%	Sensitivity% (95% CI)	Specificity% (95% CI)	*P*
$\%\Delta IU_p$	0.691 (0.582, 0.787)	>17.39	64.71 (46.5, 80.3)	70.59 (56.2, 82.5)	.001
$\%\Delta IU_d$	0.624 (0.512, 0.727)	>22.00	47.06 (29.8, 64.9)	84.31 (71.4, 93.0)	.061
$\%\Delta TIU_p$	0.796 (0.695, 0.876)	>60.80	85.29 (68.9, 95.0)	68.63 (54.1, 80.9)	<.001
$\%\Delta TIU_d$	0.780 (0.677, 0.863)	>62.19	76.47 (58.8, 89.3)	66.67 (52.1, 79.2)	<.001

Threshold was chosen according to the point nearest to the upper left corner in the ROC curves.
AUC, the area under the receiver operator characteristic curve; CI, confidence interval.

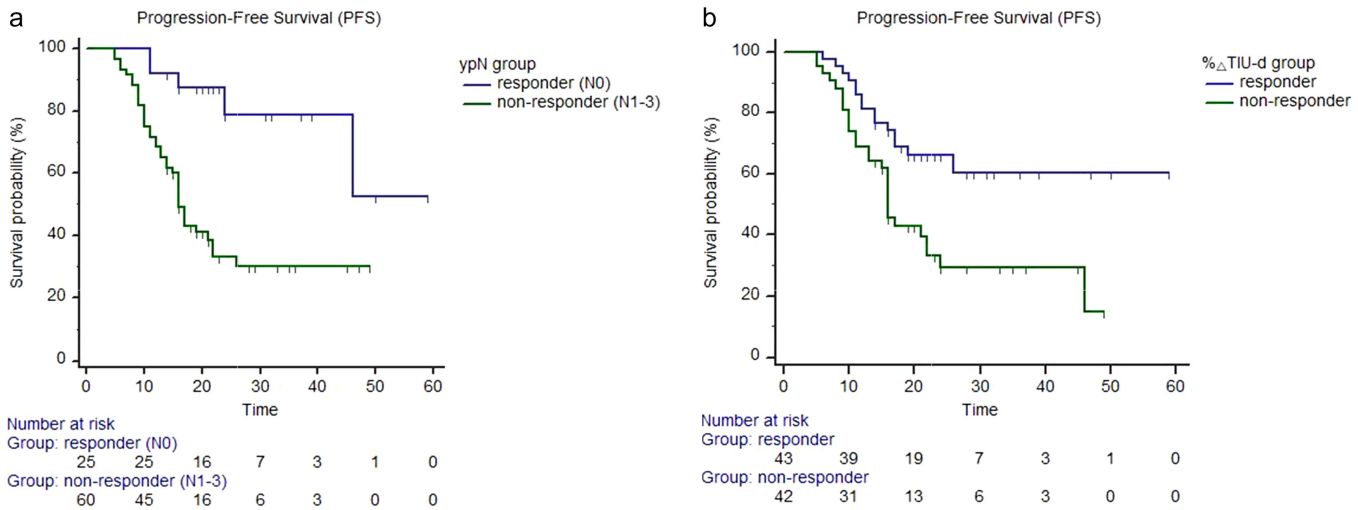

Figure 3. a, b. **(a)** Progression-free survival of N_0 versus N_{1-3} according to pathologic N staging; **(b)** Progression-free survival of responders versus non-responders according to the threshold of $\%\Delta TIU_d$ calculated by ROC analysis.

Table 4. Results of univariable analysis for progression-free survival

	Responders			Non-responders				
Parameter	N	Mean (95%CI)	SE	N	Mean (95%CI)	SE	HR (95% CI)	*P*
Sex	30	31.788 (23.027, 40.550)	4.470	55	30.284 (25.040, 35.528)	2.675	0.901 (0.481, 1.688)	.736
Age	46	36.068 (28.822, 43.314)	3.697	39	27.329 (21.384, 33.273)	3.033	1.348 (0.738, 2.463)	.315
ypT	30	38.163 (28.982, 47.344)	4.684	55	26.992 (21.933, 32.051)	2.581	1.739 (0.938,3.225)	.102
ypN	25	46.792 (37.799, 55.786)	4.589	60	24.314 (19.712, 28.916)	2.348	4.549 (2.453, 8.435)	.000*
Histological subtype	40	30.574 (24.679, 36.470)	3.008	45	33.303 (26.057, 40.550)	3.697	0.852 (0.468, 1.548)	.591
$\%\Delta IU_p$	37	34.314 (28.330, 40.299)	3.053	48	29.463 (22.569, 36.356)	3.517	1.741 (0.957, 3.166)	.073
$\%\Delta IU_d$	24	33.473 (26.524, 40.422)	3.546	61	30.621 (24.527, 36.714)	3.109	1.553 (0.805, 2.999)	.226
$\%\Delta TIU_p$	45	37.263 (30.013, 44.513)	3.699	40	25.413 (19.572, 31.253)	2.980	1.829 (0.996, 3.360)	.041*
$\%\Delta TIU_d$	43	41.385 (34.090, 48.681)	3.722	42	23.589 (18.374, 28.804)	2.661	2.361 (1.293, 4.310)	.005*

Sex (female vs. male), age (>60 y vs. ≤60 y), ypT (stage T_{0-3} vs. stage T_{4a-4b}), ypN (stage N_0 vs. stage N_{1-3}), and histological subtype (differentiated vs. undifferentiated) were divided into responders and non-responders according to the criteria in parentheses. The 4 parameters ($\%\Delta IU_p$, $\%\Delta IU_d$, $\%\Delta TIU_p$, and $\%\Delta TIU_d$) were divided into responders and non-responders according to the threshold, respectively.
N, the number of patients; SE, standard error; HR, hazard ratio; CI, confidence interval.
* represents $P < .050$.

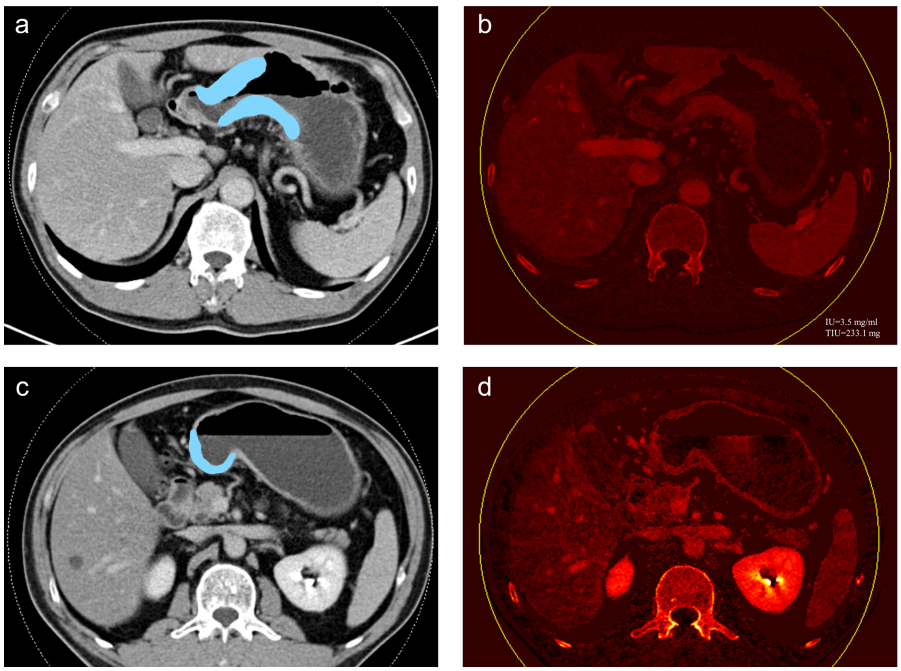

Figure 4. a-d. A 60-year-old male with undifferentiated gastric adenocarcinoma was deemed as a responder. DECT images before **(a, b)** and after **(c, d)** chemotherapy included mixed energy images **(a, c)** of delayed phase and corresponding iodine maps **(b, d)**. The tumor regression grade was grade 1, and this patient was assigned to the responder group on base of the corresponding thresholds of $\%\Delta IU_p$ (52.78%), $\%\Delta IU_d$ (57.14%), $\%\Delta TIU_p$ (93.49%) and $\%\Delta TIU_d$ (94.90%), respectively. Finally, this patient survived progression free for 14 months.

The TIU, with a more significant decrease than that of the IU, was observed in our study for monitoring treatment response and evaluating potential prognostic value. With DECT and semi-automatic post-processing techniques, TIU measurements are easy and robust to perform. Quantified TIU indirectly provides information about the microvascular environment,[33,34] thus reflects the vascularization.[35] Moreover, TIU could provide more accurate information about blood perfusion and vascularization and the perfusion of iodine contrast agents in vital tumors directly affects the amount of TIU. Therefore, it can more directly and sensitively reflect these intratumor changes caused by NAC.

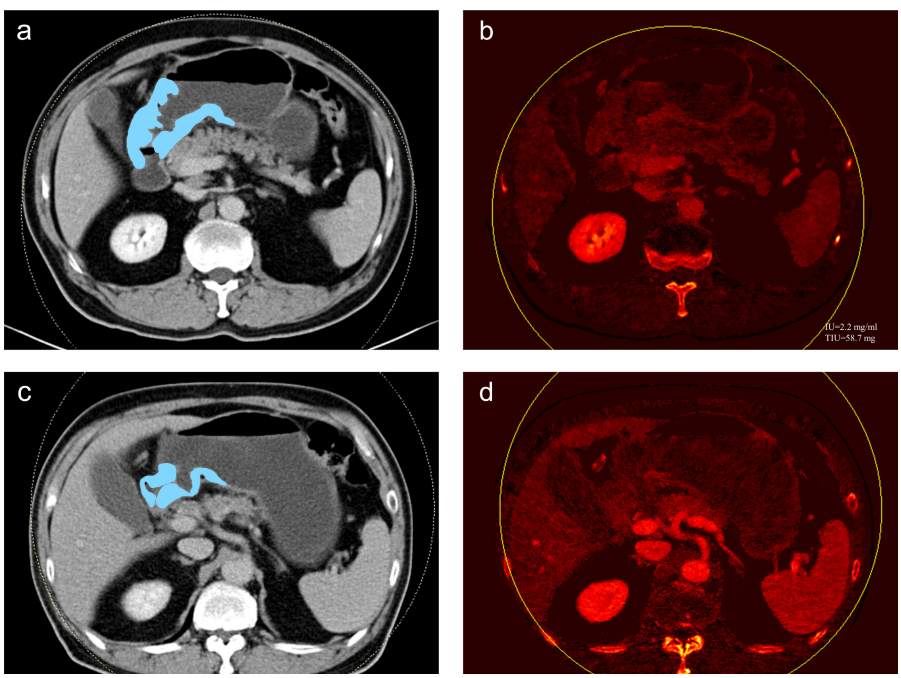

Figure 5. a-d. A 71-year-old male with differentiated gastric adenocarcinoma was deemed as a nonresponder. DECT images before **(a, b)** and after **(c, d)** chemotherapy included mixed energy images **(a, c)** of delayed phase and corresponding iodine maps **(b, d)**. The tumor regression grade was grade 2, and this patient was assigned to the nonresponder group on base of the corresponding thresholds of $\%\Delta IU_p$ (0.00%), $\%\Delta IU_d$ (9.10%), $\%\Delta TIU_p$ (14.05%) and $\%\Delta TIU_d$ (24.19%), respectively. Finally, this patient presented with distant metastases after 9 months.

Although both $\%\Delta TIU_p$ and $\%\Delta TIU_d$ were significant for the evaluation of potential prognostic value, only $\%\Delta TIU_d$ was an independent prognostic factor for PFS. This finding can be explained as follows. The microvessel density (MVD) in tissues is commonly used as a biomarker of angiogenesis.[36] In primary GC, 1 study demonstrated that iodine values were proportional to MVD.[37] Specifically, iodine values at early enhancement phase correlated with MVD at relatively early-stage and well-differentiated GC, while iodine values at late enhancement phase correlated with MVD at relatively advanced-stage and poorly differentiated GC.[37] Under such conditions, TIU_d may be better correlated with the MVD in LAGC. In addition, several studies[38-40] have shown that the enhancement pattern of GC displays delayed enhancement and that it is easier to observe the lesion in the delayed phase.

Our study had some limitations. On one hand, the sample of this study was from a single institution (n = 85). Future studies with larger study populations should be performed to validate our results. On the other hand, the processing time for iodine values measurement, especially the TIU, was relatively long for each patient. We think that skilled operation and software improvements can significantly reduce the time spent during measurement. However, we believe that our results provide ample prima facie evidence that $\%\Delta TIU_p$ and $\%\Delta TIU_d$ show promise in evaluating the potential prognostic value of LAGC after NAC. In addition, further studies with different types of DECT scanners could be necessary to validate and generalize our findings.

In conclusion, iodine values (especially the TIU) are noninvasive quantitative parameters that are potentially helpful for evaluating the treatment response and survival prognosis of LAGC after NAC. $\%\Delta TIU_d$ represents a strong independent prognostic factor and improves performance for preoperative risk assessment.

Acknowledgments

The authors would like to acknowledge Zilai Pan (Department of Radiology, Ruijin Hospital, Shanghai Jiao Tong University School of Medicine) for proofreading and revising this manuscript.

Conflict of interest disclosure

The authors declared no conflicts of interest.

References

1. Torre LA, Bray F, Siegel RL, Ferlay J, Lortet-Tieulent J, Jemal A. Global cancer statistics, 2012. *CA Cancer J Clin*. 2015;65(2):87-108. [CrossRef]
2. Siegel RL, Miller KD, Jemal A. Cancer statistics, 2018. *CA Cancer J Clin*. 2018;68(1):7-30. [CrossRef]
3. Coccolini F, Montori G, Ceresoli M, et al. Advanced gastric cancer: what we know and what we still have to learn. *World J Gastroenterol*. 2016;22(3):1139-1159. [CrossRef]
4. Ychou M, Boige V, Pignon JP, et al. Perioperative chemotherapy compared with surgery alone for resectable gastroesophageal adenocarcinoma: an FNCLCC and FFCD multicenter phase III trial. *J Clin Oncol*. 2011;29(13):1715-1721. [CrossRef]
5. van Hagen P, Hulshof MC, van Lanschot JJ, et al. Preoperative chemoradiotherapy for esophageal or junctional cancer. *N Engl J Med*. 2012;366(22):2074-2084. [CrossRef]
6. Eto K, Hiki N, Kumagai K, et al. Prophylactic effect of neoadjuvant chemotherapy in gastric cancer patients with postoperative complications. *Gastric Cancer*. 2018;21(4):703-709. [CrossRef]
7. Huang ZH, Hua D, Li LH, Zhu JD. Prognostic role of p53 codon 72 polymorphism in gastric cancer patients treated with fluorouracil-based adjuvant chemotherapy. *J Cancer Res Clin Oncol*. 2008;134(10):1129-1134. [CrossRef]
8. Kim MH, Zhang X, Jung M, et al. Immunohistochemistry biomarkers predict survival in Stage II/III gastric cancer patients: from a prospective clinical trial. *Cancer Res Treat*. 2019;51(2):819-831. [CrossRef]
9. Wu S, He H, Liu H, et al. C-C motif chemokine 22 predicts postoperative prognosis and adjuvant chemotherapeutic benefits in patients with stage II/III gastric cancer. *Oncoimmunology*. 2018;7(6):e1433517. [CrossRef]
10. Han Y, Cai H, Ma L, et al. Expression of orphan nuclear receptor NR4A2 in gastric cancer cells confers chemoresistance and predicts an unfavorable postoperative survival of gastric cancer patients with chemotherapy. *Cancer*. 2013;119(19):3436-3445. [CrossRef]
11. Grenader T, Waddell T, Peckitt C, et al. Prognostic value of neutrophil-to-lymphocyte ratio in advanced oesophago-gastric cancer: exploratory analysis of the REAL-2 trial. *Ann Oncol*. 2016;27(4):687-692. [CrossRef]
12. Chen L, Yan Y, Zhu L, et al. Systemic immune-inflammation index as a useful prognostic indicator predicts survival in patients with advanced gastric cancer treated with neoadjuvant chemotherapy. *Cancer Manag Res*. 2017;9:849-867. [CrossRef]
13. Smyth EC, Fassan M, Cunningham D, et al. Effect of pathologic tumor response and nodal status on survival in the Medical Research Council adjuvant gastric infusional chemotherapy trial. *J Clin Oncol*. 2016;34(23):2721-2727. [CrossRef]
14. Schmidt T, Sicic L, Blank S, et al. Prognostic value of histopathological regression in 850 neoadjuvantly treated oesophagogastric adenocarcinomas. *Br J Cancer*. 2014;110(7):1712-1720. [CrossRef]
15. Schneider PM, Metzger R, Schaefer H, et al. Response evaluation by endoscopy, rebiopsy, and endoscopic ultrasound does not accurately predict histopathologic regression after neoadjuvant chemoradiation for esophageal cancer. *Ann Surg*. 2008;248(6):902-908. [CrossRef]
16. Karçaaltıncaba M, Aktaş A. Dual-energy CT revisited with multidetector CT: review of principles and clinical applications. *Diagn Interv Radiol*. 2011;17(3):181-194. [CrossRef]
17. Graser A, Johnson TR, Chandarana H, Macari M. Dual energy CT: preliminary observations and potential clinical applications in the abdomen. *Eur Radiol*. 2009;19(1):13-23. [CrossRef]
18. Gao X, Zhang Y, Yuan F, et al. Locally advanced gastric cancer: total iodine uptake to predict the response of primary lesion to neoadjuvant chemotherapy. *J Cancer Res Clin Oncol*. 2018;144(11):2207-2218. [CrossRef]
19. Cunningham D, Allum WH, Stenning SP, et al. Perioperative chemotherapy versus surgery alone for resectable gastroesophageal cancer. *N Engl J Med*. 2006;355(1):11-20. [CrossRef]
20. Uhrig M, Sedlmair M, Schlemmer HP, Hassel JC, Ganten M. Monitoring targeted therapy using dual-energy CT: semi-automatic RECIST plus supplementary functional information by quantifying iodine uptake of melanoma metastases. *Cancer Imaging*. 2013;13(3):306-313. [CrossRef]
21. Sano T, Aiko T. New Japanese classifications and treatment guidelines for gastric cancer: revision concepts and major revised points. *Gastric Cancer*. 2011;14(2):97-100. [CrossRef]
22. Becker K, Mueller JD, Schulmacher C, et al. Histomorphology and grading of regression in gastric carcinoma treated with neoadjuvant chemotherapy. *Cancer*. 2003;98(7):1521-1530. [CrossRef]
23. Becker K, Langer R, Reim D, et al. Significance of histopathological tumor regression after neoadjuvant chemotherapy in gastric adenocarcinomas: a summary of 480 cases. *Ann Surg*. 2011;253(5):934-939. [CrossRef]
24. Japanese Gastric Cancer Association. Japanese gastric cancer treatment guidelines 2014 (ver. 4). *Gastric Cancer*. 2017;20(1):1-19. [CrossRef]
25. Knobloch G, Jost G, Huppertz A, Hamm B, Pietsch H. Dual-energy computed tomography for the assessment of early treatment effects of regorafenib in a preclinical tumor model: comparison with dynamic contrast-enhanced CT and conventional contrast-enhanced single-energy CT. *Eur Radiol*. 2014;24(8):1896-1905. [CrossRef]
26. Jiang C, Yang P, Lei J, et al. The application of iodine quantitative information obtained by dual-source dual-energy computed tomography on chemoradiotherapy effect monitoring for cervical cancer: a preliminary study. *J Comput Assist Tomogr*. 2017;41(5):737-745. [CrossRef]
27. Giganti F, Orsenigo E, Esposito A, et al. Prognostic role of diffusion-weighted MR imaging for resectable gastric cancer. *Radiology*. 2015;276(2):444-452. [CrossRef]
28. Pan Z, Zhang H, Yan C, et al. Determining gastric cancer resectability by dynamic MDCT. *Eur Radiol*. 2010;20(3):613-620. [CrossRef]
29. Hasegawa S, Yoshikawa T, Shirai J, et al. A prospective validation study to diagnose serosal invasion and nodal metastases of gastric cancer by multidetector-row CT. *Ann Surg Oncol*. 2013;20(6):2016-2022. [CrossRef]
30. Giganti F, Marra P, Ambrosi A, et al. Pre-treatment MDCT-based texture analysis for therapy response prediction in gastric cancer: comparison with tumour regression grade at final histology. *Eur J Radiol*. 2017;90:129-137. [CrossRef]
31. Yoon SH, Kim YH, Lee YJ, et al. Tumor heterogeneity in human epidermal growth factor Receptor 2 (HER2)-positive advanced gastric cancer assessed by CT texture analysis: association with survival after trastuzumab treatment. *PLoS ONE*. 2016;11(8):e0161278. [CrossRef]
32. Lubner MG, Smith AD, Sandrasegaran K, Sahani DV, Pickhardt PJ. CT Texture analysis: definitions, applications, biologic correlates, and challenges. *RadioGraphics*. 2017;37(5):1483-1503. [CrossRef]
33. Agrawal MD, Pinho DF, Kulkarni NM, Hahn PF, Guimaraes AR, Sahani DV. Oncologic applications of dual-energy CT in the abdomen. *RadioGraphics*. 2014;34(3):589-612. [CrossRef]
34. Kaza RK, Platt JF, Cohan RH, Caoili EM, Al-Hawary MM, Wasnik A. Dual-energy CT with single- and dual-source scanners: current applications in evaluating the genitourinary tract. *RadioGraphics*. 2012;32(2):353-369. [CrossRef]
35. Baxa J, Matouskova T, Krakorova G, et al. Dual-phase dual-energy CT in patients treated with erlotinib for advanced non-small cell lung cancer: possible benefits of iodine quantification in response assessment. *Eur Radiol*. 2016;26(8):2828-2836. [CrossRef]
36. Blank S, Deck C, Dreikhausen L, et al. Angiogenic and growth factors in gastric cancer. *J Surg Res*. 2015;194(2):420-429. [CrossRef]
37. Chen XH, Ren K, Liang P, Chai YR, Chen KS, Gao JB. Spectral computed tomography in advanced gastric cancer: can iodine concentration non-invasively assess angiogenesis? *World J Gastroenterol*. 2017;23(9):1666-1675. [CrossRef]
38. Tsurumaru D, Miyasaka M, Nishimuta Y, et al. Differentiation of early gastric cancer with ulceration and resectable advanced gastric cancer using multiphasic dynamic multidetector CT. *Eur Radiol*. 2016;26(5):1330-1337. [CrossRef]
39. Pan Z, Zhang H, Yan C, et al. Determining gastric cancer resectability by dynamic MDCT. *Eur Radiol*. 2010;20(3):613-620. [CrossRef]
40. Lee DH, Seo TS, Ko YT. Spiral CT of the gastric carcinoma: staging and enhancement pattern. *Clin Imaging*. 2001;25(1):32-37. [CrossRef]